

A novel distributed feedback fiber laser accelerometer

WANG Rui, WANG Yong-jie, LI Fang, LIU Yu-liang

Optoelectronic System Laboratory, Institute of Semiconductors, Chinese Academy of Sciences,
Beijing 100083, P.R.China

ABSTRACT

A novel distributed feedback fiber laser accelerometer based on silicon rubber is developed. The unique mechanism employed for the accelerometer ensures uniform strain distribution on the fiber laser's Bragg element. A mathematical model of single-degree-of-freedom system is established, giving the expression of the sensitivity and resonant frequency of the accelerometer. A multiple-degree-of-freedom simulation with finite element method is also conducted, giving a more precise prediction of accelerometer's characteristic. Several accelerometers of this type are constructed and tested. The wavelength shift signal is demodulated using phase generated carrier technique. The experimental result shows they have a sensitivity of 72 pm/G and a resonant frequency of 415Hz, which agree well with the simulation results. The minimum detectable signal of the whole sensing system is about 1.5 μ g. The accelerometer's structure is simple and the components employed are all commercially available, indicating a great potential in practical use.

Keywords: distributed feedback fiber laser, accelerometer, optical accelerometer, finite element method

1. INTRODUCTION

Fiber optic accelerometers are currently the focus of considerable research attention due to a number of perceived benefits over conventional piezo-electric accelerometers including reduced weight and cost, high reliability, and low power budgets [1-2]. The more recent emergence of distributed feedback fiber laser (DFB FL) offers the promise of a new generation of intra-fiber optical accelerometer [3-4]. The wavelength of light produced by DFB FL is extremely sensitive to small perturbations in its surrounding environment. It is believed that strains as small as 10^{-14} result in a measurable change to the laser wavelength [5]. Besides, DFB FL is inherently suited to array multiplexing, making it attractive for large-scale applications [6]. DFB FL accelerometers can be used in situations such as condition monitoring, downwell seismic, and security.

In this paper, a novel DFB FL accelerometer is presented. It consists of a silicon rubber cylinder and a mass. The symmetrical structure of the accelerometer offers a unique mechanism that makes sure the Bragg element of the laser is uniformly tensioned. By adjusting the structural parameters, this type of accelerometer achieves both relatively high sensitivity and high resonance frequency, showing a great promise in future applications.

2. BASIC PRINCIPLE

The structure of a DFB FL accelerometer is illustrated in Fig.1. A silicon rubber has its surface rigidly fixed to a metallic mass and base, which is done during the rubber molding process. A tiny slot in the middle of the rubber cylinder is made to facilitate the wrapping of the DFB FL and ensures the consistency of accelerometers. A preloaded DFB FL is wrapped in the slot of the rubber cylinder, with the point where two fibers cross glued, forming a closed fiber coil. When outside vibration signals stimulate the base, the mass pushes and pulls the rubber, resulting in a tangential strain in the rubber cylinder which couples into the fiber coil and modulates the wavelength of the DFB FL. A phase-generated carrier (PGC) [7] technique is used to demodulate this wavelength shift signal. The DFB FL accelerometer has a simple structure, and the components are all commercial products. That means the accelerometer is at low cost and has potential in large-scale applications.

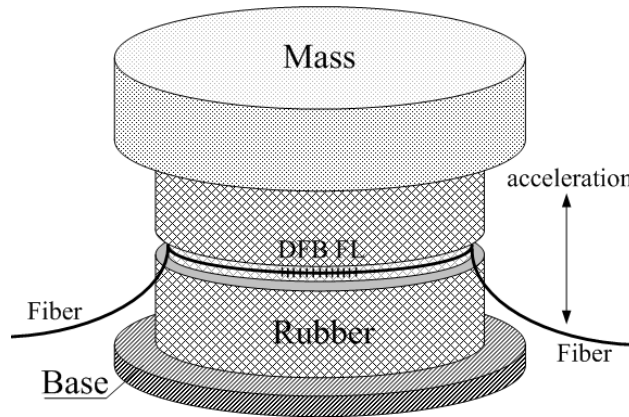


Fig. 1. Schematic diagram of a DFB FL accelerometer.

3. THEORETICAL ANALYSIS AND FINITE ELEMENT METHOD SIMULATION

Before analyzing, a few assumptions have to be made. First, small displacement and low-frequency are required because the whole analysis and simulation is based on a linear elastic theory. Second, the effect of the fiber coil on the rubber cylinder is neglected due to its much smaller stiffness compared with the rubber cylinder.

3.1 Dynamic analysis based on elastic theory

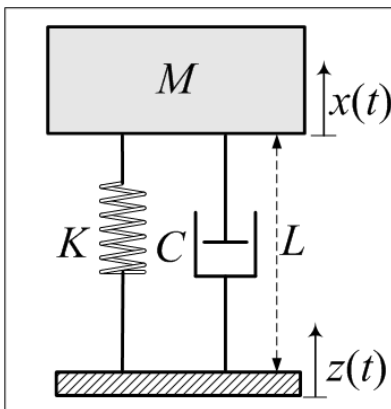


Fig. 2. A single-degree-of-freedom model for the DFB FL accelerometer.

The DFB FL accelerometer described here is based on a single-degree-of-freedom system, which can be established as shown in Fig.2. In this model the elastic rubber cylinder is equivalent to an idea spring, K , C and L are its stiffness, damping coefficient and length. M is the mass. $z(t)$ and $x(t)$ are respectively the displacement of the mass and the base.

According to Newton's second law, the dynamical equation of this system can be established as

$$M \frac{d^2 z}{dt^2} + C \left(\frac{dx}{dt} - \frac{dz}{dt} \right) + K(x - z - x_0) + Mg = 0 \quad (1)$$

where x_0 is the initial displacement of the mass loading on the rubber, thus, $Kx_0 = Mg$. The relative movement $z_r(t)$ is the most important in this analysis, $z_r(t) = x(t) - z(t)$. Then equation (1) can be expressed as

$$M \frac{d^2 z_r}{dt^2} - C \left(\frac{dz_r}{dt} \right) - Kz_r = M \frac{d^2 x}{dt^2} \quad (2)$$

Assume outside stimulating signal is cosinoidal

$$x(t) = d \cos(wt) \quad (3)$$

where d is the amplitude of the signal, then acceleration a of this signal can be given by

$$a = \frac{d^2 x}{dt^2} = -w^2 d \cos(wt) \quad (4)$$

Combining equation (3) and (2), the stable solution $z_r(t)$ could be given by

$$z_r = A \cos(wt - \varphi) \quad (5)$$

where φ is a phase delay. A and φ is given by

$$A = \frac{d\bar{\omega}^2}{\sqrt{(1-\bar{\omega}^2)^2 + (2\xi\bar{\omega})^2}} \quad \varphi = \arctan\left(\frac{2\xi\bar{\omega}}{1-\bar{\omega}^2}\right) \quad (6)$$

where the damp ratio ξ , frequency ratio $\bar{\omega}$ and the resonant frequency w_n are given by

$$\xi = \frac{C}{2\sqrt{MK}} \quad \bar{\omega} = \frac{w}{w_n} \quad w_n = \sqrt{\frac{K}{M}} \quad (7)$$

The parameter K can be calculated according to the basic elastic theory

$$K = \frac{\pi ED^2}{4L} \quad (8)$$

where D is the diameter of the rubber cylinder, E is the elastic modulus.

From equation (6), it can be seen that the amplitude response is dependent on the frequency of outside stimulating signal, it climbs when the frequency is approaching the system's resonant frequency f_0 , which can be obtained by solving the system's free vibrational equation

$$f_0 = \frac{1}{4} \sqrt{(1-\xi^2) \frac{ED^2}{\pi LM}} \quad (9)$$

However, when $\xi \ll 1$ and $\bar{\omega} \ll 1$, there will be

$$\frac{1}{\sqrt{(1-\bar{\omega})^2 + (2\xi\bar{\omega})^2}} \rightarrow 1 \quad \varphi \rightarrow 0 \quad (10)$$

Then $z_r(t)$ could be simplified as

$$z_r(t) \approx d\bar{\omega}^2 \cos(wt) = -\frac{1}{w_n^2} \frac{dx^2}{dt^2} = -\frac{4ML}{\pi ED^2} a \quad (11)$$

It can be seen that the relative displacement z_r is proportional to the acceleration a , which is the basic working principle of accelerometers. z_r causes a axial strain ε_z on the rubber, $\varepsilon_z = z_r/L$. According the elastic theory, for isotropic materials, $\varepsilon_\varphi = \nu\varepsilon_z$, where ε_φ is the tangential strain.

The tangential strain on the surface of the rubber cylinder couples into the DBF FL. The wavelength-shift response $\Delta\lambda$ of the DBF FL can be represented by the expression.

$$\Delta\lambda = \lambda(1-P)\varepsilon_\varphi \quad (12)$$

where λ is the wavelength of the DFB FL, P is the photonic elastic coefficient. The acceleration sensitivity of DFB FL accelerometer S thus can be given by

$$S = |\Delta\lambda|/a = \lambda(1-P)\nu \frac{4M}{\pi ED^2} \quad (13)$$

From expression (9) and (13), it can be seen that decreasing the cylinder length L can increase the system's resonant frequency f_0 without affecting sensitivity S . However, this dynamic model neglects the boundary conditions that the rubber cylinder has its two ends rigidly constrained by the metal plate. As L get smaller, the constrained bound will significantly increase the stiffness of the whole sensing element, thus decrease the sensitivity. So compromise between the sensitivity and the resonant frequency has to be made.

The elastic cylinder is made of silicone rubber, which can keep stable mechanical characteristics in a wide range of temperature, therefore ensuring the accelerometer performs well in tough situations. The elastic modulus, Poisson ratio and damping ratio of the rubber are 7.5 MPa, 0.48 and 0.07. Equation (9) and (13) indicate the proposed accelerometer has a sensitivity of 83 pm/G and a resonant frequency of 357 Hz, when $M=75$ g, $\lambda=1550$ nm, $L=14$ mm, $D=30$ mm.

3.2 Modal analysis using finite element method

In the above theory, formulas of accelerometer's sensitivity and resonant frequency is given to describe idea responses of the system stimulated along the axial of the accelerometer with relatively low frequency, however, the whole transducer is a multi-degree system, in which many vibration modes with different shapes and frequencies can exist. In fact, the deviation between the accelerometer produced and designed is inevitable. What's more, practical vibration signal is multiple. Thus different vibration modes of the transducer might be excited, resulting that the frequency response will not be flat or predictable and the data analysis followed will be complicated.

Modal analysis is a widely used way to estimate the dynamic response of complex structure by abstract the potential vibration modes. It gives the modes' frequencies and shapes. As to the accelerometer, the undesirable vibration modes can be eliminated or greatly reduced by properly designing the structure or improving the packaging technique.

For an N-degree-of-freedom linear system, the dynamic equation can be expressed as

$$[M] \left\{ \frac{d^2 x(t)}{dt^2} \right\} + [C] \left\{ \frac{dx(t)}{dt} \right\} + [K] \{x(t)\} = \{F(t)\} \quad (14)$$

where $[M]$, $[C]$ and $[K]$ are system's mass, damping and stiffness matrixes, and $\{x\}$ and $\{F\}$ are the displacement and stimulating force vectors.

In the modal analysis, the stimulating force is zero. And for the rubber material, the damping is rather small, thus can be omitted. Then equation (14) can be simplified as

$$[M] \left\{ \frac{d^2 x(t)}{dt^2} \right\} + [K] \{x(t)\} = 0 \quad (15)$$

Then $\{x\}$ can be expressed as

$$\{x(t)\} = \{x_0\} \sin(\omega t + \varphi) \quad (16)$$

where ω is resonant frequency, φ is initial phase. Combining equation (15) and (16), there is

$$\{[K] - \omega^2 [M]\} \{x_0\} = 0 \quad (17)$$

$\{x_0\}$ can be non-zero only if

$$\det\{[K] - \omega^2 [M]\} = 0 \quad (18)$$

The solution $\omega_i (i=1:N)$ is the natural frequency of i th mode of the system, and $\{x(t)\}$ represents the corresponding mode shape.

Finite element (FE) simulation is a most frequently used method for modal analysis and in this paper we analyze the system's modal characteristics by means of FE software ANSYS.

The transducer is modeled with twenty-node hexahedron solid element, as in Fig.3. The rubber cylinder has much more dense grid than the mass and supporting plate. The parameter of the rubber material is the same as that used in the theoretical analysis. The mass and the supporting plate are copper cylinder with diameters of 35mm and 40mm, heights

of 9.2mm and 2mm, and a density of 8500kg/m³. The displacement of the nodes on the lower surface of the supporting plate is constrained, since it is fixed to housing package.

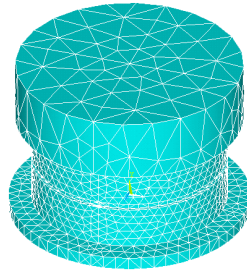


Fig. 3. FE model of the DFB FL accelerometer.

The first five modes are depicted in Fig.4. The fourth mode is the mode hoped to be excited, however, there are three vibration modes with frequencies below it. That means these modes which might be potential noise sources need to be suppressed, especially the first and third modes. In these two modes, the placement of the rubber in the slot is not uniform, causing strain in the DFB FL and ruining the sensing characteristics. By special packaging technique, these modes can be suppressed. In the second mode, there is torsion in the rubber cylinder, but no change of the slot's circumference. That means the wavelength of DFB FL is not affected. The fifth mode has a vibration frequency which is far away from the working frequency band, and therefore it is very hard to be excited and can be neglected. It also can be seen the resonant frequency predicted in FE method is higher than that given by theoretical analysis.

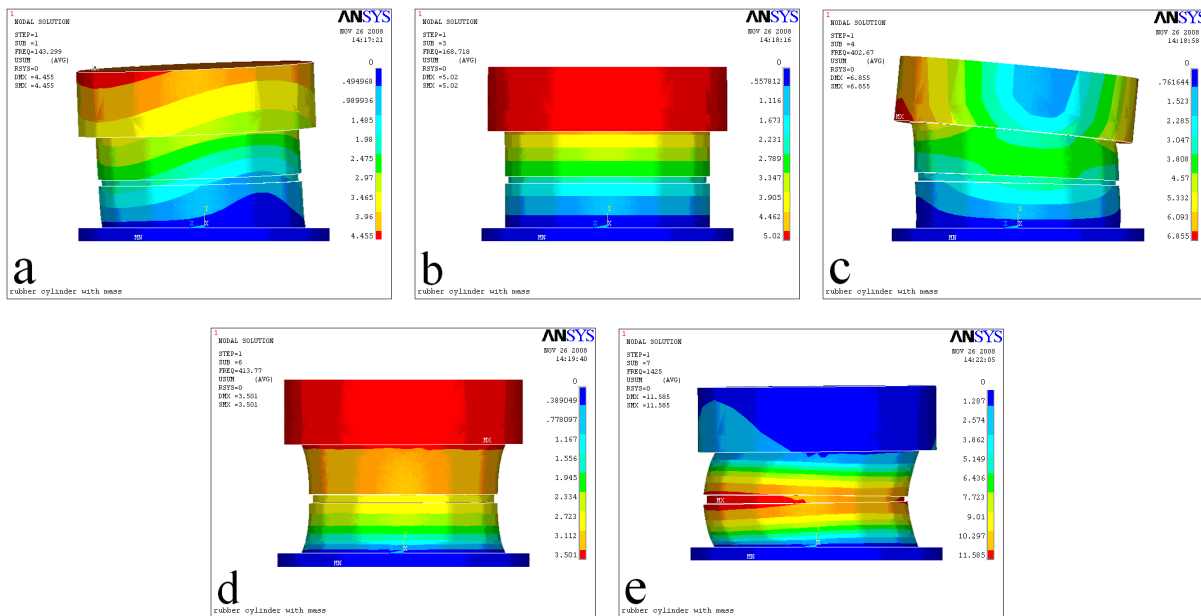


Fig. 4. (a) First modal shape, 143Hz, the rubber cylinder along with mass swinging off symmetry axis.
 (b) Second modal shape, 169Hz, the rubber cylinder along with mass twisting about symmetry axis.
 (c) Third modal shape, 403Hz, the mass swinging in radial direction.
 (d) Fourth modal shape, 414Hz, the mass pulling and pushing the rubber cylinder.
 (e) Fifth modal shape, 1425Hz, the rubber cylinder protruding.

4. EXPERIMENTAL RESULTS AND DISCUSSION

Four accelerometers with the parameters used in the FE simulation are fabricated and packaged properly, as shown in Fig.5. The laser wavelengths are chosen to be different on the purpose of future multiplexing, varying from 1530 to

1537nm. A fixed tension on the DFB FL is applied by passing one fiber end over a pulley and applying a hanging weight of 50g. The measurement setup is illustrated in Fig.6, including mainly a shaker and a digital PGC demodulator. The DFB FL is optically pumped using a laser operating at 980 nm with an optical power of 200 mW via a WDM coupler working at 980 nm/1550 nm. Through the return port of the WDM coupler, the light emitted by the DFB FL enters the input of an all-fiber Mach-Zehnder interferometer with a free space path imbalance of 5 m. A piezoelectric transducer (PZT) is incorporated into one of the arms of the interferometer to facilitate passive signal processing techniques by modulating the interferometer to induce a phase-shift carrier signal at the photo detector output. The DFB FL accelerometer along with a piezoelectric accelerometer taken as a reference are placed on the shaking table and excited over the frequency band of 10-500Hz.

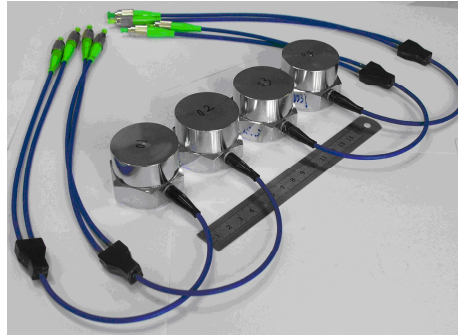


Fig. 5. Photo of DFB FL accelerometers.

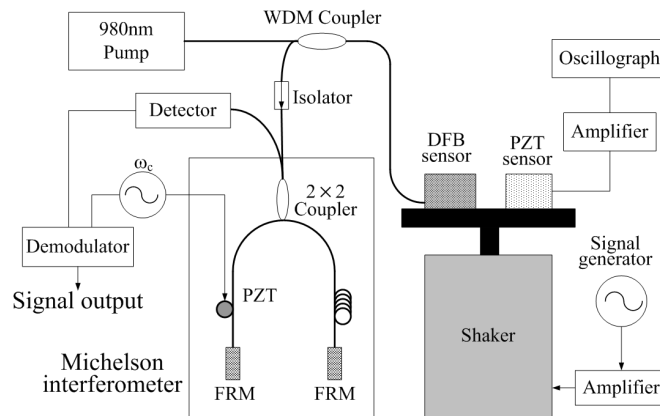


Fig. 6. Diagram of the measurement setup. (PZT: piezoelectric transducer; FRM: Faraday rotation mirror)

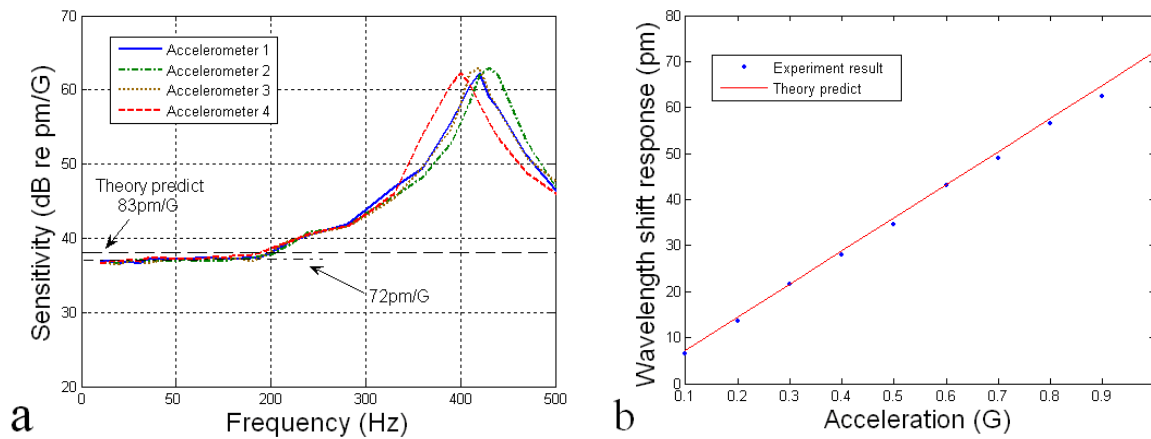


Fig. 7. (a) Frequency responses of four accelerometers. (b) Wavelength shift response with different acceleration.

The frequency response of the accelerometers is shown in the Fig.7a. It can be seen that below 200Hz, the sensitivity is 72 pm/g, and the response curve is rather flat. The resonant frequency is about 415 Hz, close to the FE method simulation predict. These measured results of four accelerometers are consistent with each other. Fig.7b shows that the wavelength shift responses have a good linear relationship with the accelerations, also agreeing well with the Theory. The noise of the whole sensing system is about 1×10^{-4} pm/ $\sqrt{\text{Hz}}$, thus its minimum detectable acceleration reaches 1.5 μg in theory.

5. CONCLUSIONS

A novel DFB FL accelerometer based on a rubber cylinder is presented. Theoretical analysis and FE method simulation are conducted. Analytical formulas of the sensitivity and resonant frequency are provided for tailing the design parameters to various applications. Four accelerometers of this type are fabricated and tested, showing a sensitivity of 72 pm/G and resonant frequency of 415Hz, which agrees well with the simulation result. The mechanism employed here ensures uniform strain distribution on the Bragg grating element and consistency of accelerometers' performance. The accelerometer is simply constructed with commercial parts, thus it can be produced at low cost and used in large-scale areas, offering a great promise in future.

REFERENCES

- [1] K.T.V. Grattan and T. Sun, "Fiber optic sensor technology: an overview," *Sens. Actuators A*, 82, 40-61 (2000).
- [2] Y.J. Rao, "Recent progress in applications of in-fibre Bragg grating sensors," *Opt. Lasers Eng*, 31, 297-324 (1999).
- [3] S. Foster, A. Tikhomirov, M. Milnes, J. van Velzen and G. Hardy, "A fibre laser hydrophone," *Proc. SPIE 5855*, 627-630 (2005).
- [4] D. J. Hill, B. Hodder, J. D. Freitas, S. D. Thomas and L. Hickey, "DFB fibre-laser sensor developments," *Proc. SPIE 5855*, 904-907 (2005).
- [5] K. P. Koo and A. D. Kersey, "Fibre laser sensor with ultrahigh strain resolution using interferometric interrogation," *Electron. Lett.*, 31, 1180-1182 (1995).
- [6] K. P. Koo and A. D. Kersey, "Noise and cross talk of a 4 element serial fiber laser sensor array," in *Proc. Opt. Fiber Commun.*, 266-267 (1999).
- [7] Y Anthony Dandridge, Alan B. Teeten and Thomas G. Giallorenzi, "Homodyne demodulation scheme for fiber optic sensors using phase generated carrier," *IEEE Transactions on Microwave Theory and Techniques*, 30, 1635-1641 (1982).